Biomedical Microdevices 3:3, 245–254, 2001

Design and Fabrication of CD-like Microfluidic Platforms for Diagnostics: Microfluidic Functions

Marc J. Madou,[1] L. James Lee,[2] Sylvia Daunert,[3] Siyi Lai,[2] and Chih-Hsin Shih[2]*

[1]Department of Materials Science and Engineering
[2]Department of Chemical Engineering The Ohio State University Columbus, Ohio 43210
[3]Department of Chemistry University of Kentucky

Abstract. **In this paper, the design of a polymer based microfluidic compact disk (CD) platform is presented. Several microfluidic functions such as flow sequencing, cascade micro-mixing, and capillary metering can be integrated into the CD by balancing the centrifugal force and the capillary force. These functions are demonstrated experimentally. For flow sequencing, a two-point calibration design is used as an example to show how the release and flow of fluids can be precisely controlled by the rotation speed of the CD. For cascade micro-mixing, a typical application is reconstituting lyophilized protein. A simple metering technique based on bubble snap-off in the two-phase flow is also described.**

Key Words. **microfluidic, centrifugal force, capillary force, CD platform, flow sequencing, micro-mixing, sample metering**

Introduction

Current trends in biomedical diagnostics and drug discovery suggest a rapid growth in the need for high speed and high throughput chemical detection, screening, and compound synthesis. The main drawbacks of the existing technologies are their reliance on expensive instruments and large sample volume, a lack of portability, and an incomplete integration of sample processing. To accelerate drug delivery and therapeutics, contain high health care costs, and provide decentralized biomedical diagnostics (i.e., diagnostics for point-of-care), future technologies are moving towards increased miniaturization, integration, and automation. Microinstrumentation that is based on integrating large parallel arrays of miniaturized fluidic systems and sensors can greatly reduce reagent volume and sample contamination. It can also provide faster and more efficient compounding and separations in biomedical and analytical applications. Tasks that are now performed in a series of conventional benchtop instruments can be combined into a single portable unit [1].

The major technical challenges in making a miniature biomedical instrument include: design and implementation of necessary microfluidic functions; integration of these functions with complete automation; and development of cost-effective manufacturing technology [2]. Microfluidics is the manipulation of fluids in channels, with at least two dimensions at the micron scale. It is a core technology in a number of miniaturized systems developed for chemical, biological, and medical applications [3]. A wide range of microfluidic components such as pumps, valves, mixers, and flow sensors has been demonstrated [4]. The main challenge in making miniaturized systems is the integration of different microfluidic components to perform certain functions at high speed and high throughput. Integrated microfluidic systems have the potential for applications such as microreaction technology, on-chip flow-through-PCR, bio-separation, clinical diagnostics, drug discovery and delivery, lab-on-a-chip technology, air bag triggers, and ink jet nozzles [5].

In this paper, we describe a compact disk (CD)-like microfluidic platform for biomedical diagnostics applications [6]. The CD platform integrates a number of microfluidic functions. By spinning the disk, the centrifugal force overcomes the capillary force and the fluid is pumped from the center towards the edge of the disc. Control of fluid transfer from one reservoir to another is achieved by manipulating the spin velocity of the disc. By coupling the CD drive with a detection system, samples on the CD can be analyzed (e.g., based on adsorption or fluorescence). This microfluidic CD platform has the advantages of low-cost, easy operation, parallel detection, fast response suitable for point-of-care, and minimum sample usage (usually in sub-microliter range). A user only needs to place a drop of sample (e.g., blood or urine) on the CD, and a computer with a CD reader does the rest of the work. The user can also transmit the results via the Internet to the hospital or doctor's office for medical consultation or for storing the data in a central data bank.

*Corresponding author.

Specifically, the CD platform consists of a disposable plastic cartridge (disk) incorporating the reagents needed for a set of tests and a separate permanent instrument (reader) [6]. The disc contains the fluid-handling manifold, other special fluidic functions, the chemistries (e.g., necessary clinical reagents and proteins) in either liquid or dried form, and CD-ROM format information. All instrumentation and control systems such as power, spindle motor, heaters, actuators for any valves, and the detection system are contained in the reader. The focus of this paper is on the design of microfluidic functions. The development of polymer based microfabrication methods is given in Part II [7].

Microfluidic Functions

In order to study how fluids flow inside micron-sized channels used in the CD platforms, a series of experiments was carried out using a Newtonian fluid, double-distilled water, and a non-Newtonian fluid, 7% bovine serum albumin (BSA) solution. The BSA solution shows shear thinning behavior (i.e., its viscosity decreases as the shear rate increases). A syringe pump (ISCO Model 100DM) was used as the pumping unit. The inlet of the pump is connected to a reservoir and the outlet of the pump is connected to a microchannel cell. An inline filter (Valco Instrument) is installed to filter the contaminant in the liquid. A pressure transducer (PX302-300GV, OMEGA) is connected right before the inlet of the cell to monitor the inlet pressure. The flow in the microchannel is monitored by a video equipment setup. Two microchannels, one 150 μm wide and 34 μm deep and the other 50 μm wide and 34 μm deep, were fabricated on a glass plate through photolithography using SU-8 (MicroChem) as the photoresist. The microchannel is then encapsulated in a holder (the bottom part is a PMMA block and the top part is aluminum with a view window). For channels of a micron size, a flow with a very high shear rate will be produced even at very low Reynolds numbers. The pressure rise curves of water and BSA solution flowing through the two microchannels at different flow rates are shown in Figure 1. Because the shear rate inside the microchannel is so high (10^5 to 10^6 sec^{-1}), the shear thinning BSA solution actually behaves like a Newtonian liquid. The measured pressure drop vs. flow rate relationship can be predicted by the Hagan-Poisseuille equation

$$Q = \frac{\pi d_H^4 \Delta P}{128\,\mu L} \tag{1}$$

where Q is the volumetric flow rate, d_H is the hydrodynamic diameter of the channel, ΔP is the pressure drop between the inlet and outlet, μ is the viscosity of the fluid, and L is the length of the microchannel. These results indicate that, within the range of channel size used in this study, the surface forces are negligible in one-phase flow.

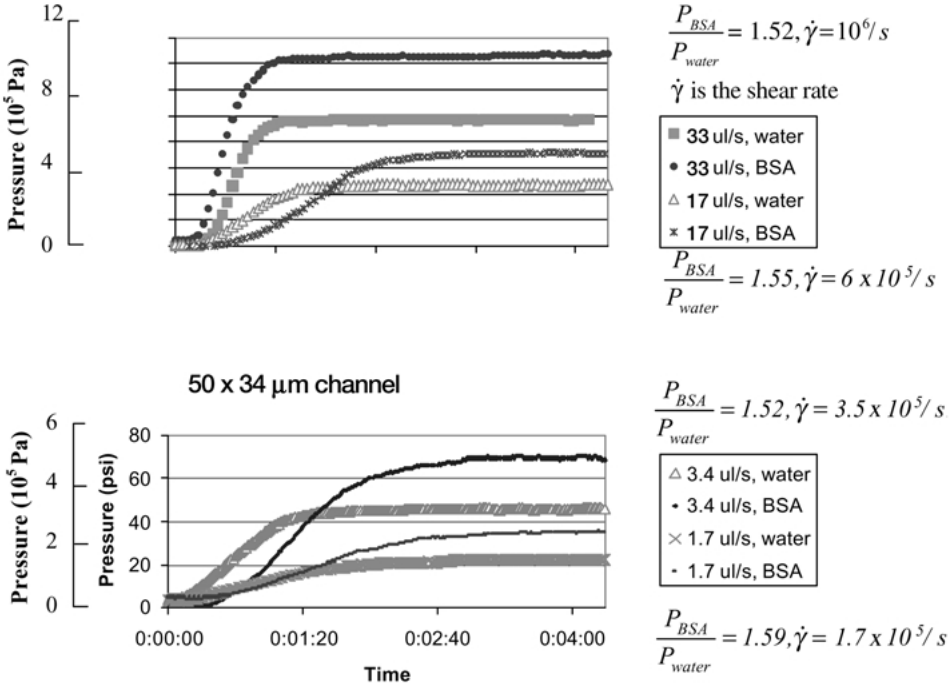

Fig. 1. *Pressure curve for flow.*

Major microfluidic components include sample introduction or loading (and in some cases, sample preparation); propulsion of fluids (such as samples to be analyzed, reagents, and wash and calibration fluids) through micron-sized channels; valving; fluid mixing and isolation as desired; small volume sample metering; sample splitting and washing; and temperature control of the fluids. In this study, we focus our effort on the design of three microfluidic functions by manipulating both centrifugal and capillary forces on the CD platform. Flow sequencing and washing are achieved by centrifuge-based fluid propulsion and capillary valving. A cascade micro-mixing design allows sequential mixing on the CD. A simple technique based on bubble snap-off in the two-phase flow can be used for small volume metering.

Flow sequencing by centrifugal propulsion and capillary valving

Various microfluidic propulsion technologies have been reviewed and compared by Madou et al. [6,8] with regard to the choice of materials, the maturity of the technology, and the achievable volumetric flow rates. In general, the fluid propulsion can be generated mechanically, electrically, or thermally. In the pressure-based approach, a mechanical pump is often used to provide the driving pressure. The pump can be as simple as a roller in the blister pouch design [6,9] or as complicated as a miniaturized syringe or acoustic pump [6,10]. The former is simple, low cost, and readily available, however, there is little opportunity of it for further miniaturization or for high throughput tests. The latter is costly and the choice of materials is limited to piezoelectrics for acoustic pumping. Pressure-based propulsion does have the attractive feature of being generic for the kinds of fluids that can be pumped. On the other hand, electro-kinetic techniques such as electro-osmosis or electrophoresis [11–15], electrodynamics [16,17], and electrowetting [18] have the advantage that they scale favorably for miniaturization. In electro-osmosis or electrophoresis, the driving forces for flow are generated by the interaction of applied electric fields with ionic species in the fluids. In electrodynamics, the flow is generated by the interaction of electric fields with induced electric charges in the fluids. Electrowetting is based on the principle that the contact angle between a liquid and a solid surface can be changed through the application of an electrical potential. This change may result in capillary forces that provide a driving pressure in a small flow channel. Since these techniques become more effective with decreasing volume size and increasing surface area, they are very attractive in microfluidic applications. However, they need high electric fields and depend strongly on the properties of fluids to be pumped (such as pH or charges). Many organic compounds and solvents may not be able to meet the charge and pH requirements [19]. Thermal methods can also be used for fluid propulsion. Sammarco and Burns [20] manipulated the contact angle between a liquid and a solid surface by changing the local fluid temperature. The resulting capillary force is used to drive the fluid as in electrowetting. In the case of phase-change pumping [21], the driving pressure arises from the volume change due to the phase change from liquid to gas, as the liquid is heated. Considering the high heat exchange rate in small channels, this mechanism scales well down to the microdomain. Thermal methods are still in the early research stage and they require careful control of the local temperature. By contrast, in centrifugal pumping, fluid propulsion is achieved through rotationally induced hydrostatic pressure. It is simple, uses a single low-cost motor, and is capable of fine flow control through proper design of the location, dimensions and geometry of channels and reservoirs based on fluid properties. It can also be easily integrated with the information-carrying capacity of the CD.

Another essential component in the microfluidic system is the ability to stop and start the fluid flow. Conventional diaphragm valves [20,22–24] can fulfill this task, but they usually require moving parts and an external actuation mechanism such as a change in temperature, pH or charge. Controlling the liquid flow electro-kinetically has been recently demonstrated [25]. This method, however, requires a high electric field, is sensitive to the properties of the fluids, and may lead to the occurrence of Joule heating [26]. An alternative approach is to use a passive capillary-valve that relies on the capillary force to stop the flow in micro-channels. The principle of operation is based on a pressure barrier that develops when the cross-section of the capillary expands abruptly. Capillary valving has the advantage of not requiring any moving parts and external actuation. Recently this type of valve has attracted a great deal of attention and has a strong appeal for applications in various microfluidic systems [6,8,26–28].

In our CD platform, the centrifugal force provides the pumping pressure, while the capillary force at junctions inhibits flow. This constitutes a RPM-dependent capillary ''valve'' controlling the release and flow of fluids. The two opposing forces can be described as follows (see Figure 2). The pumping force per unit area (P_c) due to the centrifugal force is given by:

$$\frac{dP_C}{dr} = \rho\omega^2 r \tag{2}$$

where ρ is the density of the liquid, ω is the angular

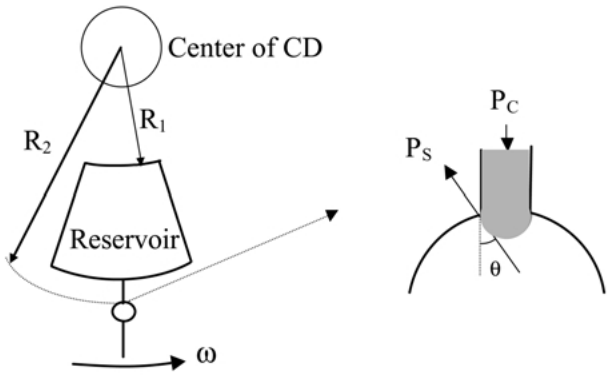

Fig. 2. Schematic illustration of fluid propulsion.

velocity of the CD platform, and r is the distance of a liquid element from the center of the CD.

Integration of equation (2) from $r = R_1$ to $r = R_2$ gives [6]:

$$\Delta P_C = \rho\omega^2(R_2 - R_1)\left(\frac{R_1 + R_2}{2}\right) = \rho\omega^2 \cdot \Delta R \cdot \overline{R} \tag{3}$$

where $\overline{R}$ is equal to $\frac{R_1+R_2}{2}$. The capillary force per unit area (P_s) due to interfacial tension is given by:

$$\Delta P_S = \frac{C\gamma\cos\theta}{A} \tag{4}$$

where γ is the surface tension of the fluid, θ is the contact angle, A is the cross-section area of the capillary, and C is the associated contact line length [6].

The liquid is released from the reservoir when ΔP_c is greater than ΔP_s. The burst frequency is the rotation speed at which fluids are released from their reservoirs. The burst frequency, f_b, calculated from equations (3) and (4) is given by:

$$f_b = \left(\frac{\gamma\cos\theta}{\pi^2\rho \cdot \Delta R \cdot \overline{R} \cdot d_H}\right)^{\frac{1}{2}} \tag{5}$$

where d_H, equal to $4A/C$, is the hydrodynamic diameter of the channel connected to the junction.

By appropriately choosing the channel dimensions and the junction size and location, precise flow sequencing can be realized.

To demonstrate this flow sequencing function, a 2-point calibration design for medical diagnostics is described here [8,28]. In this design (see Figure 3), the pre-loaded liquids should flow to the optode reservoir in the order of calibrant 1, wash 1, calibrant 2, wash 2, and the sample by increasing the rotation speed of the CD platform. The same optode reservoir is used for measuring both calibrant and sample fluids, in order to eliminate systematic errors common with devices using

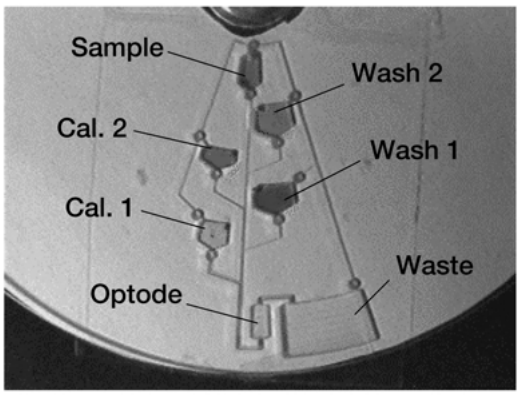

Flow order: Cal. 1➔Wash 1➔Cal. 2➔Wash 2➔Sample

Fig. 3. Two-point calibration microfluidic platform.

separate reservoirs for measuring sample and calibrates. In order to test the burst frequency of each reservoir, CNC (computerized numerically controlled)-machined polycarbonate (PC) disks, 12 cm in diameter, were made with a 2-point calibration design. Each disk was covered with a flat PC plate by Scotch tape bonding. The experimental setup for microfluidic testing is shown in Figure 4. The disk is mounted on a motor plate (up to 5000 r.p.m.) designed by Gamera Bioscience, which is connected to an encoder to trigger a strobe (Monarch, DA 115/Nova Strobe) for synchronized imaging. When the same position of the CD passes under a CCD camera (Panasonic GP-KR222), the strobe is triggered. Therefore, only a fixed position of the CD is highlighted in each turn. The image of the CD is then sent to a computer or a VCR for data storage. Figure 5 shows a series of snapshots taking during a test run. Deionized water containing different colors of food dye was used as the test fluid. At a low rotation speed (524 r.p.m.), only the calibrant 1 fluid went to the optode reservoir, while the other fluids stayed in their reservoirs. When the rotation speed increased in steps, the fluids of wash 1, calibrant 2, wash 2, and the sample moved to the optode

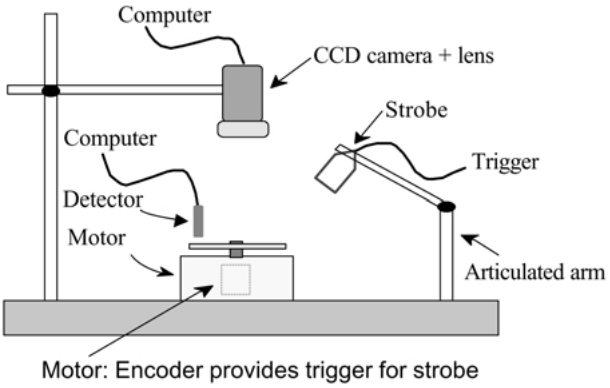

Fig. 4. Experimental setup for CD microfluidic testing.

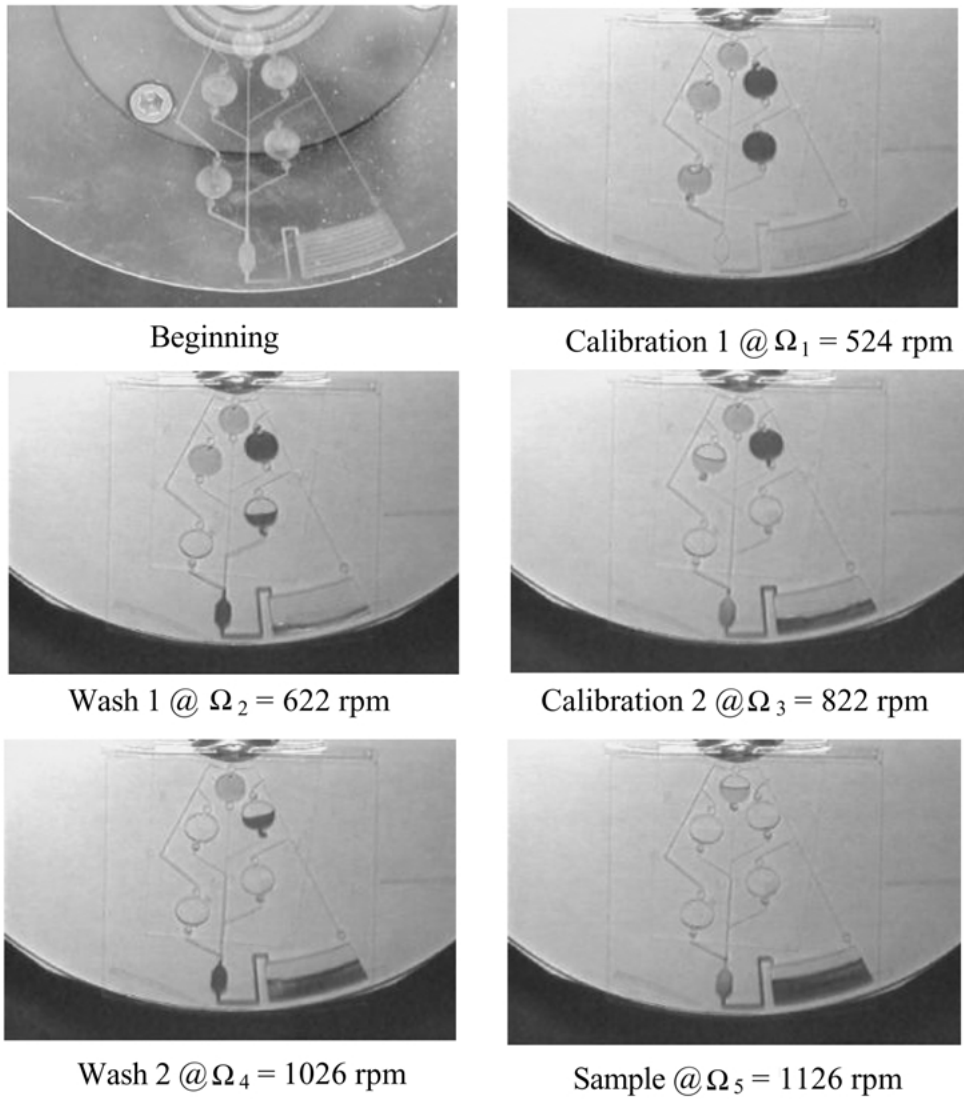

Fig. 5. *Flow sequence of a two-point calibration system.*

reservoir in the right order. By using food dye as an indicator, it was found that the volume of the incoming fluid needs to be 3 times that of the reservoir, in order to completely displace the existing fluid. For some applications, the washing solution may not be needed. However, for bio-fluids such as an enzyme solution, washing is essential because of protein binding to the polymer substrate. Table 1 summarizes the channel dimensions and burst frequencies for the experiments. Figure 6 shows the test results on two CNC-machined CDs. Considering the tolerance of CNC machining [7], the experimental results agree reasonably well with the calculated burst frequencies.

In designing the microfluidic systems, the shape of reservoirs and channels may play an important role. Figure 7 shows three designs of the 2-point calibration system. When the shape of the reservoirs was changed from rectangular, to circular, to raindrop-like, sample loading in the reservoirs became easier (i.e., less likely to trap air bubbles) and there was less liquid retained after release. Sharp corners or turns should be avoided in the design of micro-channels and reservoirs, because they tend to cause high residual stresses during disc fabrication. Among the three designs, the raindrop-shaped reservoirs provided the best performance in both microfluidic experiments and disc fabrication. In order to ensure that the optode reservoir is completely filled and washed after each displacement, the shape of the optode reservoir and the relative location of the optode reservoir and the waste reservoir are important. In Design I of Figure 7, the incoming fluid passed through the center portion of the optode reservoir, leaving dead space near the corners. In Design II, the optode width is narrower with a rounded inlet and outlet. Although good washing

Table 1. Channel dimensions and burst frequencies

	Channel dimensions (μm)		Burst frequencies (r.p.m.)	
Reservoir	Width	Depth	Calculated	Experimental
Sample	127	63.5	1222	1126
Wash 2	127	63.5	1032	1026
Calibrant 2	254	127	832	822
Wash 1	254	127	623	622
Calibrant 1	508	254	427	524

was achieved, the optode reservoir did not totally fill in some cases. In Design III, the incoming fluid moved into the optode reservoir from the bottom to the top, ensuring complete filling and washing.

Cascade micro-mixing

Because of the micron-sized flow channels, the Reynolds number of fluid flow in the microfluidic systems is extremely small (usually less than 1). The lack of turbulent flow makes the mixing in microdevices a very challenging issue. Diffusion is the main driving force in micro-mixing due to the nature of laminar flow. Design of micromixers is generally based on increasing the diffusion time, enlarging the contact area, and creating more chaotic flows.

The enlargement of the contact surface between two fluids can be achieved in many different ways. Static-type (i.e., no moving parts) micromixers based on the concept of lamination [29,30] or separation-reunification [31] have been developed and studied. A similar approach is to divide each flow into several partial flows in order to increase the contact area. Injecting one liquid into another liquid with microplumes can achieve the same goal [30,32]. The basic principle of these micromixers is to decrease the diffusion length required for mixing. Some of the static micromixer designs can be complicated, e.g., the lamination type where very precise alignment is required [33].

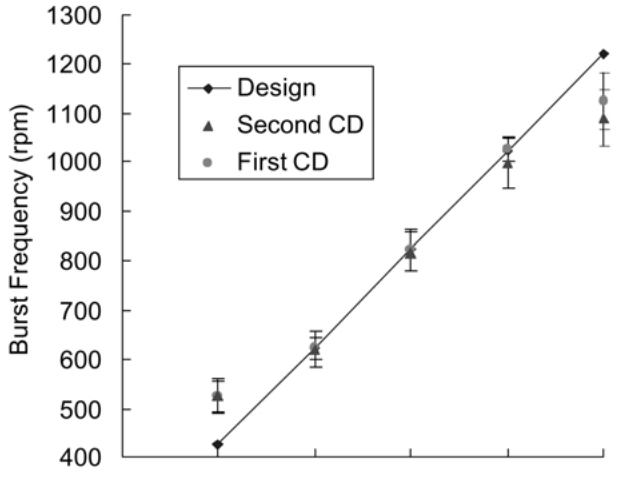

Fig. 6. Burst frequencies of the CNC-machined CD platform based on DI-water.

A chaotic flow field can be generated with two pumps connected via source and sink to a mixing chamber [34]. This design employs chaotic advection for mixing. It is more efficient than static mixers, but requires expensive instrumentation. In electro-kinetic based microfluidic systems, convective mixing can be achieved by inducing surface charges at the interface of liquid samples that have different conductivities [35]. The surface charges react with the applied electric fields to generate electric shear forces. The separate flow streams mix when passing the electrodes. Successful mixing results have been demonstrated [35]. One can also place a solid post in the middle of the micro-flow channel. By applying one electric field to the surface of the channel wall and an opposite electric field to the surface of the post, convective mixing can be achieved when the fluids pass the post. However, this kind of mixer depends on the physiochemical properties of fluids and therefore limits its general applications.

The cascade micromixer structure we designed for our CD platform is schematically shown in Figure 8a. In this design, two buffer solutions in reservoir 1 are released simultaneously at a low rotation speed, then mixed at the joint point by impingement mixing to create a chaotic flow. As in flow sequencing, the centrifugal force provides the driving pressure while the capillary valve controls the flow release. The mixture goes through an S-shaped channel. This channel increases the contact time and creates bend-induced vortices to stir the fluid and therefore enhance the mixing process [36]. The mixture then flows into reservoir 2 where a solid protein is located. Such a design reduces the contact time between proteins and buffer solutions, minimizing protein denaturing. In order to totally fill reservoir 2, the combined volume of the two buffer solutions needs to be slightly larger than the volume of reservoir 2. The excess solution enters into an overflow reservoir. After the protein is dissolved, the protein solution and a sample solution are released simultaneously at a higher rotation speed. They are also mixed by impingement mixing and

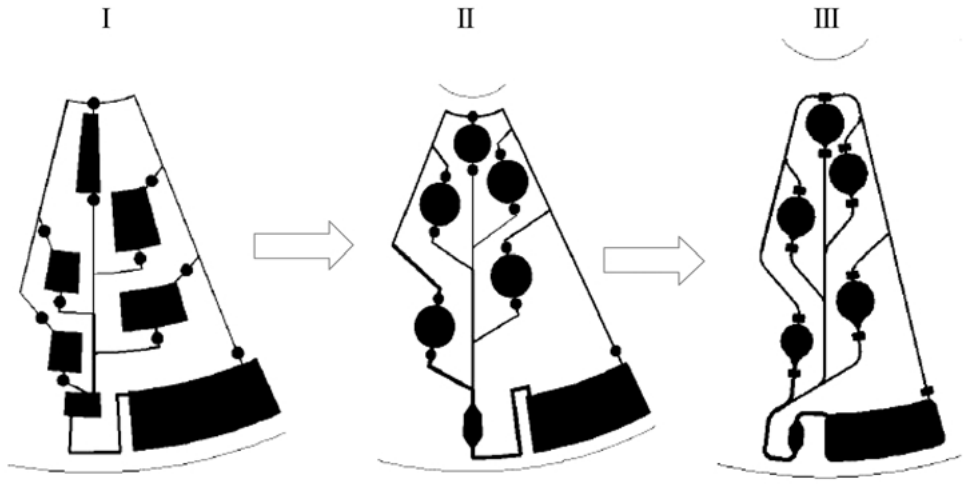

Fig. 7. *Three 2-point calibration designs.*

bend-induced vortices when flowing into the optode reservoir for detection. Figure 8b shows a snapshot of an impingement mixing experiment during mixing of two water samples containing food dyes.

Capillary metering by bubble snap-off

Delivery of precisely metered fluids from one reservoir to another in a well-controlled sequence is important in many microfluidic applications. Several methods have been developed for this purpose. An on-chip technique to meter discrete nanoliter-sized liquid drops inside microchannels was developed, using a combination of a hydrophobic surface treatment and air pressure [37]. This technique involves spontaneously filling the microchannel up to a hydrophobic stop and splitting a liquid drop by injecting air through a hydrophobic side channel. Accurate liquid volumes, ranging from 0.5 to 125 nl, were metered using this technique. Another method is to draw a liquid sample from a larger reservoir to a number of smaller capillaries and let the excess liquid flow into an overflow chamber. The capillaries containing metered liquid samples can then be released in sequential order by capillary valving as described in flow sequencing [6]. These methods, however, require fairly complicated design and implementation.

Here, we describe a simple approach to achieve

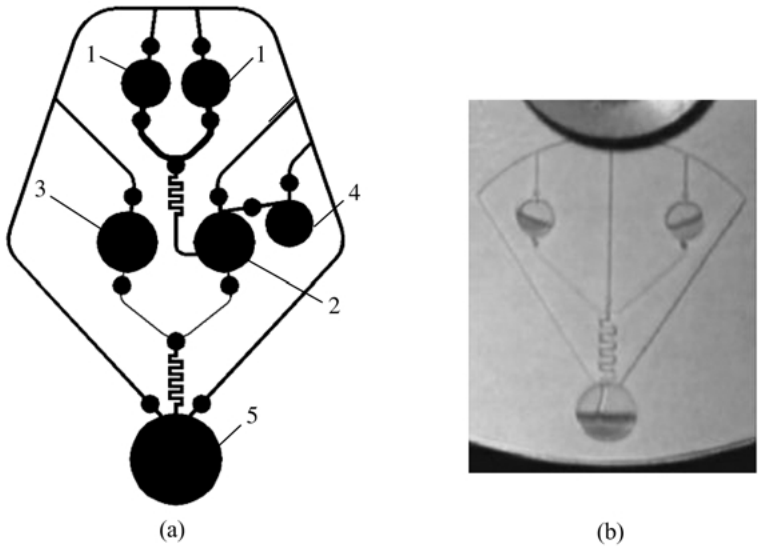

Fig. 8. *A cascade micromixer design (a) 1, buffer solution; 2, solid protein; 3, sample with analyte; 4, overflow chamber; 5, optode, and (b) during mixing.*

sample metering. When a gas bubble in the liquid-gas flow passes through a constriction, it may break up into a number of equally-spaced small bubbles. The mechanism of this ''snap-off'' phenomenon has been described by Ransohoff et al. [38]. When the gas bubble enters a constriction initially filled with a wetting liquid, the bubble front enters the downstream body, while the wetting liquid remains in the corners. The curvature and corresponding pressure at the bubble front fall with expansion of the interface. The resulting capillary pressure gradient initiates a liquid pressure gradient from the pore body toward the pore throat. Liquid is then driven along the corner into the pore-throat where it accumulates as a collar. The collar grows and snaps-off the bubble. The process of the snap-off is schematically shown in Figure 9.

This simple mechanism can be applied for sample metering in microfluidic systems because a fixed amount of liquid is trapped between two bubbles that are snapped off. For the purpose of illustration, a microchannel with a constriction was designed and fabricated as shown in Figure 10. The height of the channel was 67 μm, its width was 100 μm and the constriction width was 20 μm. It was fabricated through photolithography on a glass plate. A Newtonian fluid (silicone oil, Dow Corning 200® 500 cst.) was used in the experiments. The experimental setup was the same as for studying the fluid flow in microchannels as described previously. The flow of the air bubble inside the microchannel was monitored by a video setup. A snapshot of bubble snap-off is shown in Figure 10.

The average velocity of the gas bubble can be used to calculate the channel capillary number Ca_g:

$$Ca_g = \frac{\mu V_g}{\gamma} \tag{6}$$

where μ and γ represent the viscosity and surface tension of the liquid and V_g is the average velocity of the gas phase.

A dimensionless snap-off time τ is defined by Chambers and Radke [39] as

$$\tau = \frac{t_s \cdot \gamma}{3\mu R_T} \tag{7}$$

where t_s is the snap-off time and R_T is the channel radius (in our case, a hydrodynamic radius). The characteristic time $\frac{3\mu R_T}{\gamma}$ is defined as the rearrangement of a thin Newtonian liquid film driven by the surface tension force.

By using the dimensionless time and the capillary number based on the average gas velocity, the snap-off time vs. the channel capillary number is shown in Figure 11. A linear correlation is observed for all experimental results at different gas bubble velocities and pressures. The snap-off time can be correlated as

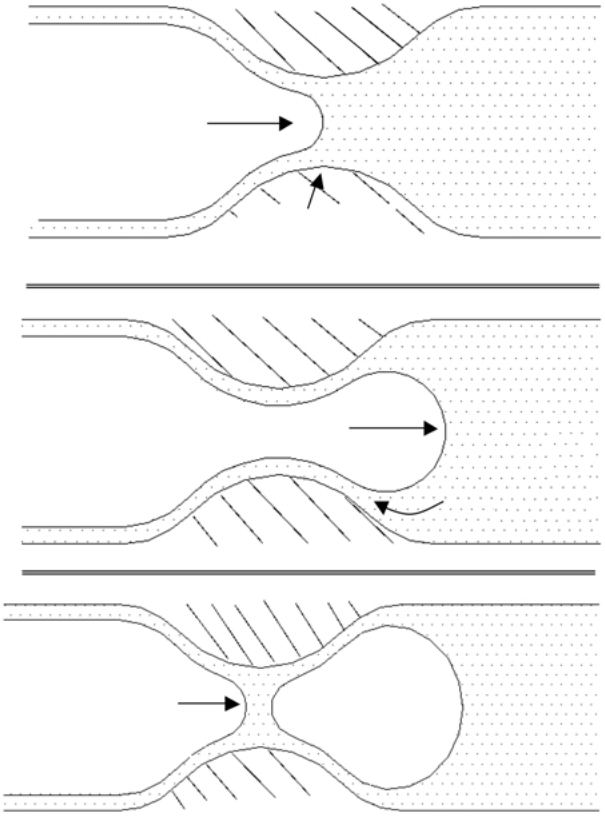

Fig. 9. Schematic of bubble snap-off from Ransohoff et al. [38].

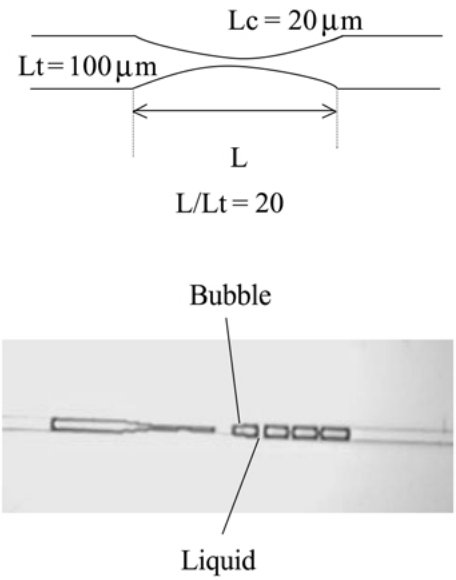

Fig. 10. A microchannel design for bubble snap-off.

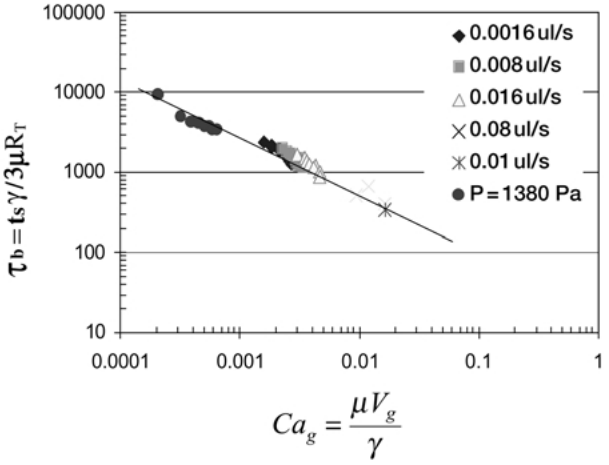

Fig. 11. *Snap-off time vs. channel capillary number based on gas velocity.*

$$\tau = F * Ca^{-0.64} \tag{8}$$

where F is a geometric factor that is equal to 33.62 in this case.

Since the distance between two metered fluid samples is determined by the snap-off time, and the liquid sample volume depends on the channel size, sample metering can be achieved by appropriately designing the geometry of the microchannel and constriction, and by controlling the channel pressure. Implementation of this metering method on the CD platform is currently underway in our lab.

Conclusions

Design of a CD-like microfluidic platform capable of a number of fluidic functions is presented. These functions have been successfully demonstrated through a series of experiments using model fluids. Their applicability to biomedical fluids is being investigated in our lab. The main issues are how non-Newtonian flow behavior will affect the centrifugal and capillary forces, and how protein binding on the channel surface will affect the capillary forces. Other microfluidic components and further miniaturization of fluidic structures are also being explored, in order to increase the functionality and capacity of the CD platform.

Acknowledgment

The authors wish to thank Greg Kellogg at Gamera Bioscience for his helpful discussions. This work is supported by NASA and the NSF Center for Industrial Sensors and Measurements (CISM) at The Ohio State University.

References

1. A. Manz, C.S. Effenhauser, N. Burggraf, E.J.M. Verpoorte, D.E. Raymond, and H.M. Widmer, Analysis Mag. **22**, M25 (1994).
2. M.J. Madou, *Fundamental of Microfabrication* (CRC Press, Boca Raton, 1997).
3. M. Freemantle, Chem. Eng. News **27**, (February 22, 1999).
4. P. Gravesen, J. Branebjerg, and O.S. Jensen, J. Micromech. Microeng. **3**, 168 (1993).
5. J.C. Mcdonald, D.C. Duffy, J.R. Anderson, D.T. Chiu, H. Wu, O.J.A. Schueller, and G.M. Whitesides, Electrophoresis **21**, 27 (2000).
6. M.J. Madou and G.J. Kellogg, SPIE Proceedings, 3259, 80, San Jose, CA (1998).
7. L.J. Lee, M.J. Madou, K.W. Koelling, S. Daunert, S. Lai, C.G. Koh, Y.-J. Juang, Y. Lu, and L. Yu, Biomedical Microdevices **3**(4) (2001, in press).
8. M.J. Madou, Y. Lu, S. Lai, L.J. Lee, and S. Daunert, Micro Total Analysis Systems, 565 (2000).
9. J.B. Findlay, S. Atwood, M.L. Bergmeyer, J. Chemelli, K. Christy, T. Cummins, W. Donish, T. Ekeze, J. Falvo, and D. Patterson, Clin. Chem. **39**, 1927 (1993).
10. R.M. Moroney, R.M. White, and R.T. Howe, IEEE 1990 Ultrasonics Symposium Proceedings, 355, Honolulu, HI (1990).
11. D.J. Harrison, Z. Fan, K. Fluri, and K. Seiler, Solid State Sensor & Actuator Workshop, 21, Hilton Head Island, SC (1994).
12. C.S. Effenhauser, G.J.M. Bruin, A. Paulus, and M. Ehrat, Anal. Chem. **69**, 3451 (1997).
13. J.R. Webster, M.A. Burns, and C.H. Mastrangelo, Annu. Int. Conf. Micro Electro Mech. Syst., Proc., 13th, 306 (2000).
14. M. Deshpande, K.B. Greiner, J. West, J.R. Gilber, L. Bousse, and A. Minalla, Solid State Sensor and Actuator Workshop, 128 (2000).
15. H.C. Chang, D.T. Leighton, A.E. Miller, A.E. Ostafin, and P.V. Takhistov, AIChE Annual Meeting, Los Angeles, CA, (2000).
16. A. Richter, A. Plettner, K. Hoffmann, and H. Sandmaier, IEEE Micro Electro Mechanical Systems (MEMS'91), 271, Nara (1991).
17. S.C. Jacobson, R. Hergenroder, A.W. Moore, and J.M. Ramsey, Solid State Sensor and Actuator Workshop, 65, Hilton Head Island, SC (1994).
18. E. Colgate and H. Matsumoto, J. Vac, Sci. Technol. **A8**(4), 3625 (1990).
19. H.J. Zheng and P.K. Dasgupta, Anal. Chem. **66**, 3997 (1994).
20. T.S. Sammarco and M.A. Burns, AIChE J. **45**(2), 350 (1999).
21. T.K. Jun and C.-J. Kim, J. Appl. Phys. **83**(11, Pt. 1), 5658 (1998).
22. I. Kaetsu, K. Uchida, H. Shindo, S. Gomi, and K. Sutani, Radiation Phys. Chem. **55**, 193 (1999).
23. R.H. Liu, Q. Yu, J.M. Bauer, J.S. Moore, and D.J. Beebe, Solid State Sensor & Actuator Workshop, 222, Hilton Head Island, SC, June (2000).
24. X. Cao, S. Lai, and L.J. Lee, Biomedical Microdevices **3**(2), 109 (2001).
25. S.C. Jacobson, S.V. Ermakov, and J.M. Ramsey, Anal. Chem. **71**(15), 3273 (1999).
26. J. Zeng, D. Banerjee, M. Deshpande, J. Gilbert, D.C. Duffy, and G.J. Kellogg, Micro Total Analysis Systems, 579 (2000).
27. D.C. Duffy, H.L. Gills, J. Lin, N.F. Sheppard, and G.J. Kellogg, J. Anal. Chem. **71**, 4669 (1999).

28. M.J. Madou, Y. Lu, S. Lai, Y.-J. Juang, L.J. Lee, and S. Daunert, Solid State Sensor & Actuator Workshop, 191, Hilton Head Island, SC, June (2000).
29. J. Branebjerg, P. Gravesen, J.P. Krog, and C.R. Nielsen, Proceedings IEEE Micro Electro Mechanical Systems (MEMS), 441 (1996).
30. M. Koch, D. Chatelain, A.G.R. Evans, and A. Brunnschweiler, J. Micromech. Microeng. **8**, 123 (1998).
31. N. Schwesinger, T. Frank, and H. Wurmus, J. Micromech. Microeng. **6**(1), 99 (1996).
32. M. Elwenspoek, T.S.J. Lammerink, R. Miyake, and J.H.J. Fluitman, J. Micromech. Microeng. **4**, 227–245 (1994).
33. P. Woias, K. Hauser, and E. Yacoub-george, Micro Total Analysis Systems, 277 (2000).
34. J. Evans, D. Liepmann, and A.P. Pisano, Proceedings IEEE Micro Electro Mechanical Systems (MEMS), 96–101 (1997).
35. J-W Choi and C.H. Ahn, Solid-State Sensor and Actuator Workshop, 52, Hilton Head, June (2000).
36. M. Yi and H.H. Bau, ASME (MEMS) Proceedings, 489 (2000).
37. K. Handique, D.T. Burke, C.H. Mastrangelo, and M.A. Burns, Anal. Chem. **72**, 4100 (2000).
38. T.C. Ransohoff, P.A. Gauglitz, and C.J. Radke, AIChE J. **33**(5), 753 (1987).
39. K.T. Chambers and C.J. Radke, *Interfacial Phenomena in Petroleum Recovery*, N.R. Morrow, eds. (Dekker Publishers, New York, 1991).